



Met Office  
Hadley Centre



UNIVERSITÄT  
BERN  
DESCHGER CENTRE  
CLIMATE CHANGE RESEARCH



Royal Netherlands  
Meteorological Institute  
Ministry of Infrastructure and the  
Environment

# Statistical Climate Reconstruction Modelling in the EUSTACE Project

Finn Lindgren ([finn.lindgren@ed.ac.uk](mailto:finn.lindgren@ed.ac.uk))

The University of Edinburgh, Scotland

with Colin Morice, John Kennedy, and the EUSTACE team,  
David Bolin, Haavard Rue, Daniel Simpson, Elias Krainski

Modern Statistical and Machine Learning Approaches for High-Dimensional Compound Spatial Extremes

BIRS-IMAG, Granada, 7–12 May 2023

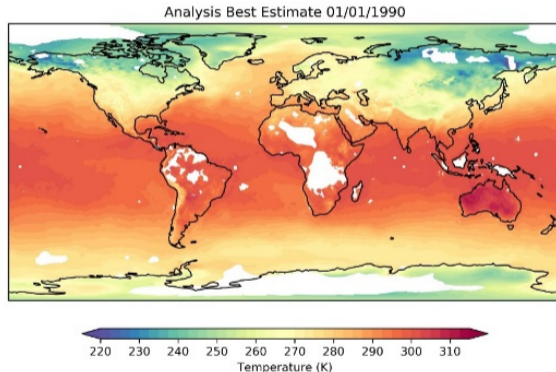
*EUSTACE has received funding from the European Union's Horizon 2020 Programme for Research and Innovation, under Grant Agreement no 640171*



# EUSTACE ANALYSIS

**Combines in-situ and satellite data sources to derive daily air temperatures across the globe with quantified uncertainties.**

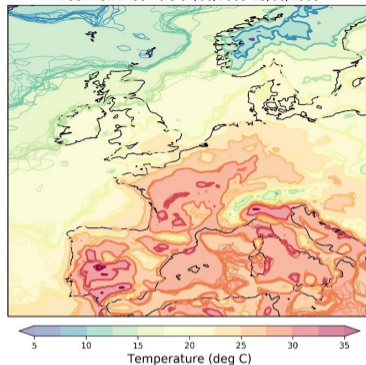
- Daily mean air temperature (2 m) estimates from the mid-late 19<sup>th</sup> century at  $\frac{1}{4}$  degree resolution.
- Observational dataset for use in climate monitoring, services and research.
  - Quantify bias and uncertainty arising from observational sampling (in space and time);
  - Quantify uncertainty from instrumental effects/network changes.
- Higher resolution daily gridded analyses for regional climate
  - Combine in situ and remote sensing data to support high resolution analysis.
  - Absolute temperature rather than anomaly product.



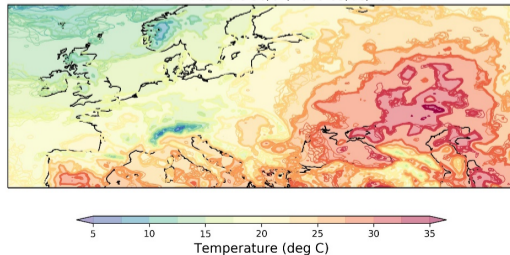
# ENSEMBLE ANALYSIS

- Samples drawn from joint posterior distribution of temperature and bias variables.
- Temperature model samples projected onto analysis grid.
- Spatial/temporal correlation in analysis errors is encoded into the ensemble.
- Summary statistics can be derived from the ensemble. Expected value, total uncertainty and observation constraint information also available.

EUSTACE Ensemble 04/08/2003-13/08/2003



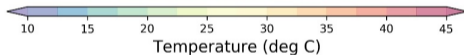
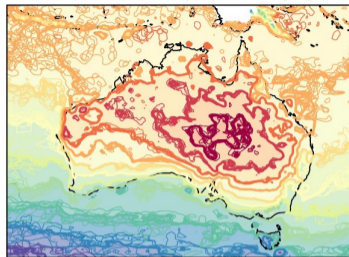
EUSTACE Ensemble 30/07/2010-05/08/2010



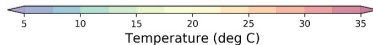
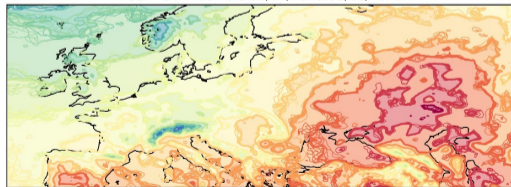
# ENSEMBLE ANALYSIS

- Samples drawn from joint posterior distribution of temperature and bias variables.
- Temperature model samples projected onto analysis grid.
- Spatial/temporal correlation in analysis errors is encoded into the ensemble.
- Summary statistics can be derived from the ensemble. Expected value, total uncertainty and observation constraint information also available.

EUSTACE Ensemble 01/01/2006-14/01/2006



EUSTACE Ensemble 30/07/2010-05/08/2010



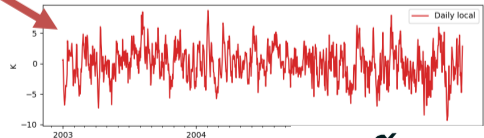
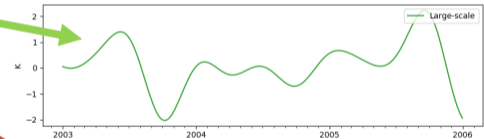
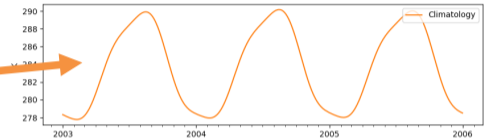
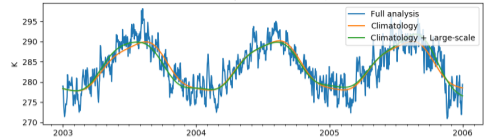
## MULTI-SCALE ANALYSIS MODEL

Statistical model for temperature variations and different scales (space and time):

- **Climatological variation**: local seasonal cycle with effects of latitude, altitude and coastal influence.
- **Large-scale variation**: Slowly varying climatological mean temperature field.
- **Daily Local**: daily variability associated with weather.

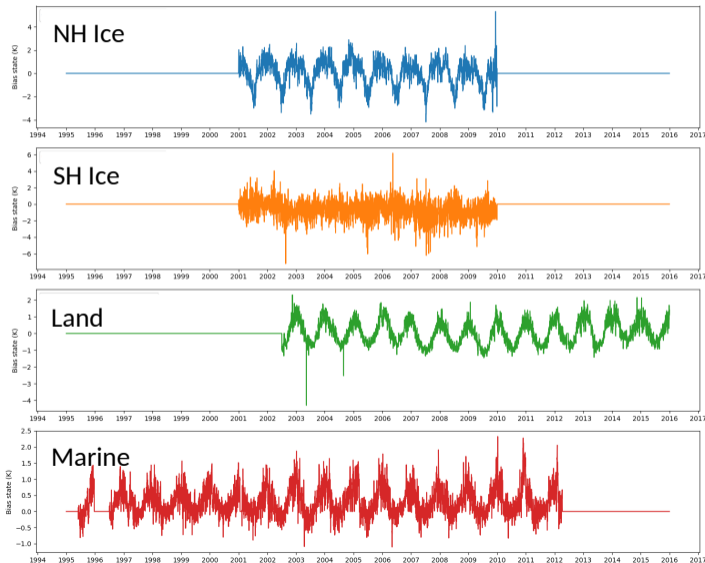
Simultaneously estimates observational biases of known bias structures:

- e.g. satellite biases, station homogenisation.

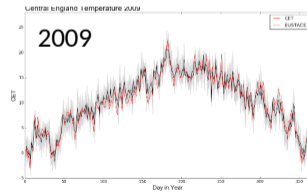
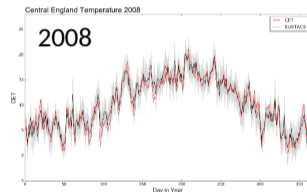
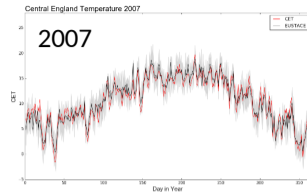
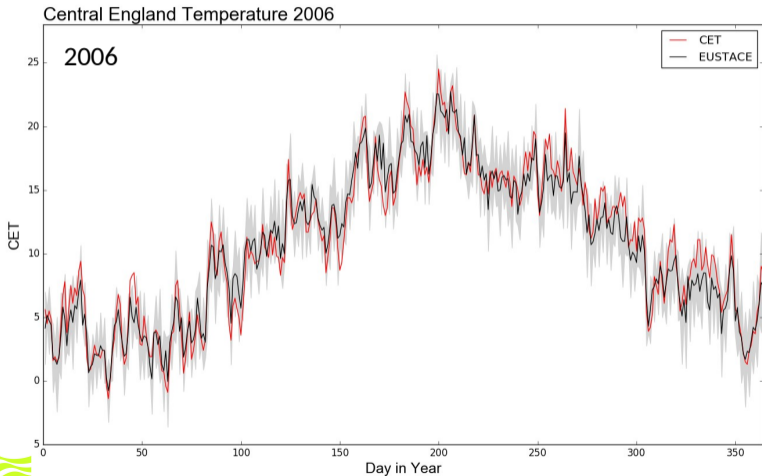


# SATELLITE BIAS MODELS

- Simplified model of known error structures in satellite air temperature retrievals:
  - Global/hemispheric systematic bias covariates.
  - Daily estimates of spatially varying bias as a spatial random field.
- Estimated jointly with daily temperature variability.



# COMPARING EUSTACE WITH CENTRAL ENGLAND TEMPERATURE



# MULTI-SCALE ANALYSIS MODEL

Statistical model for temperature variations and different scales (space and time):

- **Climatological variation:** local seasonal cycle with effects of latitude, altitude and coastal influence.
- **Large-scale variation:** Slowly varying climatological mean temperature field. Station homogenisation.
- **Daily Local:** daily variability associated with weather. Satellite retrieval biases.

Simultaneously estimates observational biases of known bias structures:

- e.g. satellite biases, station homogenisation.

Processed on STFC's LOTUS cluster [www.jasmin.ac.uk](http://www.jasmin.ac.uk):

- Largest solves processed on 20 core/256GB RAM node.
- Highly parallel observation pre-processing.

Element	Resolution	N Variables
Seasonal	Bimonthly x 1° SPDE	245,772
Slow-scale*	5 year x 5° SPDE	107,604
Latitude	0.5° latitude SPDE	721
Altitude	(0.25° grid)	1
Coastal	(0.25° grid)	1
Grand mean	Analysis mean	1

Element	Resolution	N Variables
Large-scale	3 monthly x 5° SPDE	1,752,408
Station bias	NA	82,072

Element	Resolution	N Variables per day
Daily local	~0.5 degree SPDE	162,842
Satellite bias (marine)	Global	1
Satellite bias (land)	Global + 2.5 degree SPDE	1 + 40,962
Satellite bias (ice)	Hemispheric + 2.5 degree SPDE*	2 + 40,962



# GAMs and general kriging

- ▶ Linear GAMs with GPs on space and covariates:

$$\eta_i = \sum_k f_k(z_{ik}) + u(\mathbf{s}_i),$$

each  $f_k(\cdot)$  and  $u(\cdot)$  represented with basis expansions with jointly Gaussian coefficients  $\mathbf{x}$ .

- ▶ Linear observations with additive Gaussian observation noise:  $\mathbf{y} = \boldsymbol{\eta} + \boldsymbol{\epsilon} = \mathbf{A}\mathbf{x} + \boldsymbol{\epsilon}$
- ▶ Covariance kriging

$$\begin{aligned}\boldsymbol{\Sigma}_y &= \mathbf{A}\boldsymbol{\Sigma}_x\mathbf{A}^\top + \boldsymbol{\Sigma}_\epsilon \\ \mathbb{E}(\mathbf{x}|\mathbf{y}) &= \boldsymbol{\mu} + \boldsymbol{\Sigma}_x\mathbf{A}^\top\boldsymbol{\Sigma}_y^{-1}(\mathbf{y} - \mathbf{A}\boldsymbol{\mu})\end{aligned}$$

- ▶ Precision kriging

$$\begin{aligned}\mathbf{Q}_{\mathbf{x}|\mathbf{y}} &= \mathbf{Q}_x + \mathbf{A}^\top\mathbf{Q}_\epsilon\mathbf{A} \\ \mathbb{E}(\mathbf{x}|\mathbf{y}) &= \boldsymbol{\mu} + \mathbf{Q}_{\mathbf{x}|\mathbf{y}}^{-1}\mathbf{A}^\top\mathbf{Q}_\epsilon(\mathbf{y} - \mathbf{A}\boldsymbol{\mu})\end{aligned}$$

- ▶ Non-Gaussian observations with link function:  $\mathbb{E}(y_i|\boldsymbol{\theta}, \mathbf{x}) = h(\eta_i)$

# Observation level covariance vs latent level precision

- Covariance kriging: linear solve with a  $\Sigma$ ,  $\Sigma_{ij} = \text{Cov}(y_i, y_j)$

Vecchia approximation:

$\Sigma^{-1} \approx \mathbf{L}\mathbf{L}^\top$  for a given observation ordering, and sparse lower triangular  $\mathbf{L}$  with given sparsity pattern;  
 $p(\mathbf{y}|\boldsymbol{\theta}) \approx p(y_1) \prod_{i=2}^n p(y_i|\mathbf{y}_{G_i}), G_i \subseteq \{1, \dots, i-1\},$

$$\mathbf{a}^\top \Sigma^{-1} \mathbf{a} \approx \sum_i \left( \sum_{j \in G_i} a_i L_{ij} \right)^2$$

$\mathbf{L}$  obtained sequentially from  $\Sigma$  for each observation.

- Precision kriging: linear solve with a  $\mathbf{Q}$ ,  $Q_{ij} = \text{Prec}(x_i, x_j|\mathbf{y})$

$\mathbf{Q} = \mathbf{L}\mathbf{L}^\top$  for a given latent variable ordering, and sparse lower triangular  $\mathbf{L}$  with the sparsity from  $\mathbf{Q}$  plus Cholesky infill.

The prior  $\mathbf{Q}_x$  for SPDE process components is obtained via a local Finite Element construction, giving the model in a chosen finite function space closest to the full model.

# Example model: Matérn driven heat equation on the sphere

The iterated heat equation is a simple non-separable space-time SPDE family:

$$\left[ \phi \frac{\partial}{\partial t} + (\kappa^2 - \Delta)^{\alpha_s/2} \right]^{\alpha_t} x(\mathbf{s}, t) dt = d\mathcal{E}_{(\kappa^2 - \Delta)^{\alpha_e}}(\mathbf{s}, t) / \tau$$

For constant parameters,  $x(\mathbf{s}, t)$  has spatial Matérn covariance (for each  $t$ ) in a Matérn-Whittle sense on  $\mathbb{S}^2$ .

## Discrete domain Gaussian Markov random fields (GMRFs)

$\mathbf{x} = (x_1, \dots, x_n) \sim \mathcal{N}(\boldsymbol{\mu}, \mathbf{Q}^{-1})$  is Markov with respect to a neighbourhood structure  $\{\mathcal{N}_i, i = 1, \dots, n\}$  if  $Q_{ij} = 0$  whenever  $j \notin \mathcal{N}_i \cup i$ .

- Project the SPDE solution space onto local basis functions:  
random Markov dependent basis weights (Lindgren et al, 2011).

A finite element approximation has structure

$$x(\mathbf{s}, t) = \sum_{i,j} \psi_i^{[s]}(\mathbf{s}) \psi_j^{[t]}(t) x_{ij}, \quad \mathbf{x} \sim \mathcal{N}(\mathbf{0}, \mathbf{Q}^{-1}), \quad \mathbf{Q} = \sum_{k=0}^{\alpha_t + \alpha_s + \alpha_e} M_k^{[t]} \otimes M_k^{[s]}$$

even, e.g., if the spatial scale parameter  $\kappa$  is spatially varying.



# Classic and compact INLA methods ( $\sim$ description)

- ▶ Laplace approximation at the conditional posterior mode  $\mathbf{x}^*$ , and uncertainty integration:

$$p(\boldsymbol{\theta}|\mathbf{y}) \propto \frac{p(\boldsymbol{\theta})p(\mathbf{x}|\boldsymbol{\theta})p(\mathbf{y}|\boldsymbol{\theta}, \mathbf{x})}{p(\mathbf{x}|\boldsymbol{\theta}, \mathbf{y})} \Big|_{\mathbf{x}=\mathbf{x}^*} \approx \frac{p(\boldsymbol{\theta})p(\mathbf{x}|\boldsymbol{\theta})p(\mathbf{y}|\boldsymbol{\theta}, \mathbf{x})}{p_G(\mathbf{x}|\boldsymbol{\theta}, \mathbf{y})} \Big|_{\mathbf{x}=\mathbf{x}^*} = \hat{p}(\boldsymbol{\theta}|\mathbf{y})$$
$$p(x_i|\mathbf{y}) = \int p(x_i|\boldsymbol{\theta}, \mathbf{y})p(\boldsymbol{\theta}|\mathbf{y}) d\boldsymbol{\theta} \approx \sum_k \hat{p}(x_i|\boldsymbol{\theta}^{(k)}, \mathbf{y})\hat{p}(\boldsymbol{\theta}^{(k)}|\mathbf{y})w_k = \hat{p}(x_i|\mathbf{y})$$

- ▶ Let  $\hat{\boldsymbol{\mu}} = E(\mathbf{x}|\boldsymbol{\theta}, \mathbf{y})$  and  $\mathbf{Q}_\epsilon = -\nabla_{\mathbf{x}} \nabla_{\mathbf{x}}^\top \log p(\mathbf{y}|\boldsymbol{\theta}, \mathbf{x}^*)$

- ▶ Classic method: Laplace approximation of each  $\hat{p}(x_i|\boldsymbol{\theta}, \mathbf{y})$ , and

$$\left\{ \begin{bmatrix} \mathbf{Ax} \\ \mathbf{x} \end{bmatrix} \middle| \boldsymbol{\theta}, \mathbf{y} \right\} \sim \mathcal{N} \left( \begin{bmatrix} \mathbf{A}\hat{\boldsymbol{\mu}} \\ \hat{\boldsymbol{\mu}} \end{bmatrix}, \begin{bmatrix} \mathbf{Q}_\epsilon + \delta \mathbf{I} & -\delta \mathbf{A} \\ -\delta \mathbf{A}^\top & \mathbf{Q}_x + \delta \mathbf{A}^\top \mathbf{A} \end{bmatrix}^{-1} \right), \text{ with } \delta \gg 0$$

- ▶ Compact method: Variational approximation of  $\hat{p}(\mathbf{x}|\boldsymbol{\theta}, \mathbf{y})$ , and

$$\{\mathbf{x}|\boldsymbol{\theta}, \mathbf{y}\} \sim \mathcal{N} \left( \hat{\boldsymbol{\mu}}, [\mathbf{Q}_x + \mathbf{A}^\top \mathbf{Q}_\epsilon \mathbf{A}]^{-1} \right)$$

## Before satellites you had to go measure in person



"The Discovery", Dundee, Scotland (Photos: Finn Lindgren, August 2022)

# Hydrology lab from the 1925-27 Antarctic ocean expedition



"The Discovery", Dundee, Scotland (Photos: Finn Lindgren, August 2022)

## What's that in the corner?

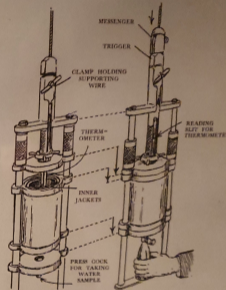


"The Discovery", Dundee, Scotland (Photos: Finn Lindgren, August 2022)

# It's a Nansen-Pettersson water sampling bottle!

## The Nansen-Pettersson water sampling bottle

Temperature and water samples down to 100m were taken with the Nansen-Pettersson water sampling bottle. The bottle is sent down on a wire to the desired depth. Then the 'Messenger' weight is sent down to close the bottle to collect the sample. The insulation helps to keep the temperature constant to allow the scientists to gather the data about the temperature using the thermometer. Water is released from the tap at the bottom for testing.



The Nansen-Pettersson water sampling bottle shown open and closed.

Diagram of the Water sampling bottle from Sir Alister Hardy's *Great Waters*.



# Station observation & homogenisation model

## Daily mean air temperature measurements

For station  $k$  at day  $t_i$ ,

$$y_m^{k,i} = T_m(\mathbf{s}_k, t_i) + \sum_{j=1}^{J_k} H_j^k(t_i) e_m^{k,j} + \epsilon_m^{k,i},$$

where  $H_j^k(t)$  are temporal step functions,  $e_m^{k,j}$  are latent bias variables, and  $\epsilon_m^{k,i}$  are independent measurement and discretisation errors.

## Daily mean/max/min

For station  $k$  at day  $t_i$ ,  $y_m^{k,i} = T_m(\mathbf{s}_k, t_i) + \tilde{H}_m^k(t_i) + \epsilon_m^{k,i}$ ,

$$y_x^{k,i} = T_m(\mathbf{s}_k, t_i) + \tilde{H}_{r,m}^k(t_i) + \frac{\tilde{H}_{r,r}^k(t_i)}{2} T_r(\mathbf{s}_k, t_i) + \epsilon_x^{k,i},$$

$$y_n^{k,i} = T_m(\mathbf{s}_k, t_i) + \tilde{H}_{r,m}^k(t_i) - \frac{\tilde{H}_{r,r}^k(t_i)}{2} T_r(\mathbf{s}_k, t_i) + \epsilon_n^{k,i},$$

where  $\tilde{H}_\cdot$  are the total bias correction variables for each observation.

# Modelling non-Gaussian quantities

## Power tail quantile (POQ) model

The quantile function  $F_{\theta}^{-1}(p)$ ,  $p \in [0, 1]$ , is defined through a quantile blend of left- and right-tailed generalised Pareto distributions:

$$f_{\theta}^{-}(p) = \begin{cases} \frac{1-(2p)^{-\theta}}{2\theta}, & \theta \neq 0, \\ \frac{1}{2} \log(2p), & \theta = 0, \end{cases}$$
$$f_{\theta}^{+}(p) = -f_{\theta}^{-}(1-p) = \begin{cases} \frac{(2(1-p))^{-\theta}-1}{2\theta}, & \theta \neq 0, \\ -\frac{1}{2} \log(2(1-p)), & \theta = 0. \end{cases}$$
$$F_{\theta}^{-1}(p) = \theta_0 + \frac{\tau}{2} [(1-\gamma)f_{\theta_3}^{-}(p) + (1+\gamma)f_{\theta_4}^{+}(p)].$$

The parameters  $\theta = (\theta_0, \theta_1 = \log \tau, \theta_2 = \text{logit}[(\gamma+1)/2], \theta_3, \theta_4)$  control the median, spread/scale, skewness, and the left and right tail shape.

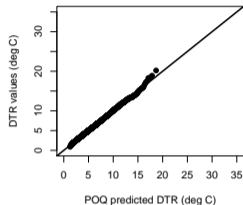
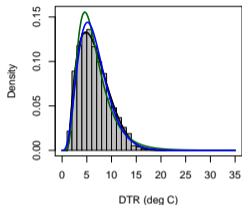
This model is also known as the *five parameter lambda model* (Gilchrist, 2000).

Transformation:  $T_r(\mathbf{s}, t) = F_{\theta(\mathbf{s}, t)}^{-1} \{ \Phi[u(\mathbf{s}, t)] \}$ ,  $E[u(\mathbf{s}, t)] = 0$ ,  $\text{Var}[u(\mathbf{s}, t)] = 1$

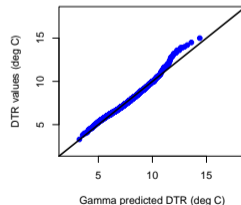
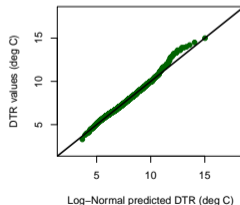
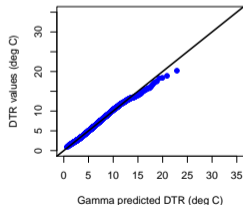
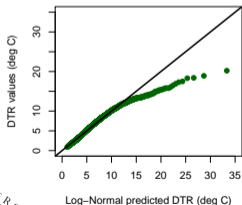
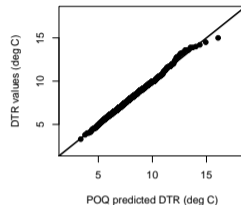
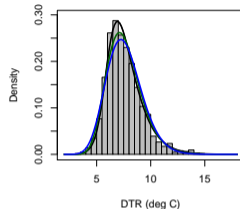


# Diurnal range distributions

RSM00025594 (BUHTA PROVIDENJA)



SP000060040 (LANZAROTE/AEROPUERT)

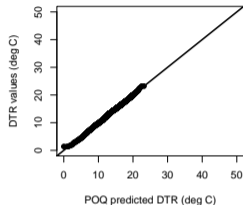
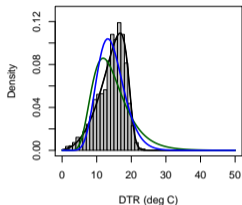


For these stations, POQ does a slightly better job than a Gamma distribution.

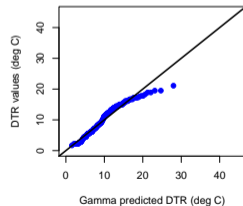
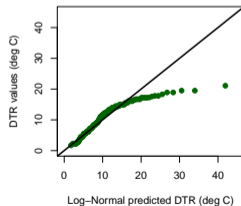
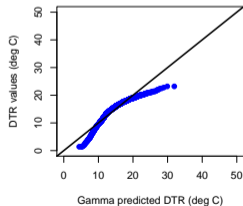
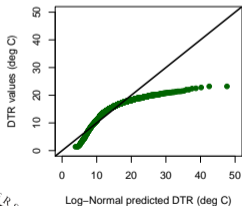
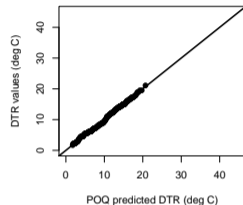
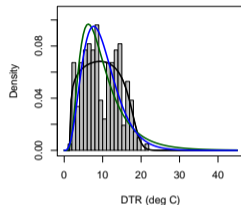


# Diurnal range distributions

ASN00005008 (MARDIE)



ASN00023738 (MYPONGA)

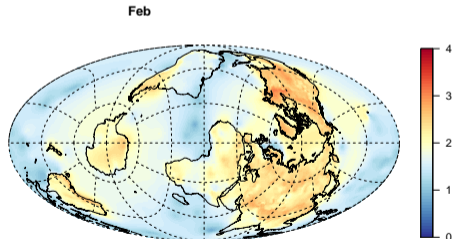
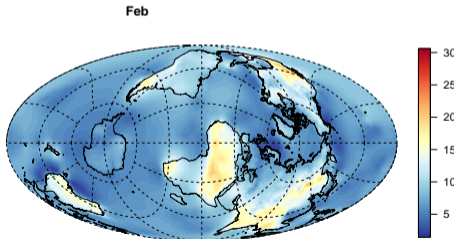
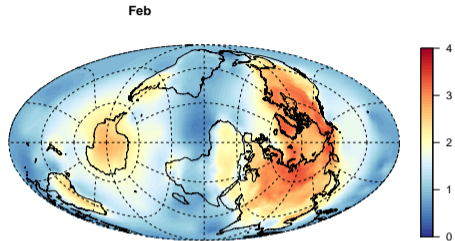
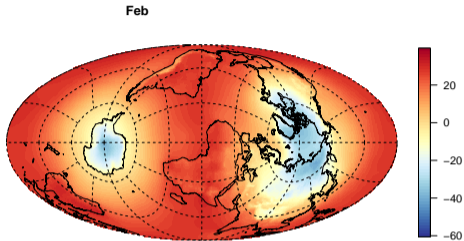


For these stations only POQ comes close to representing the distributions.

Note: Some shapes may be due to unmodeled station inhomogeneities.



# Estimates of median & scale for $T_m$ and $T_r$



February climatology

(Preliminary estimates, using only in-situ land station data)

# Linearised inference

All spatio-temporal latent random processes combined into  $\mathbf{x} = (\mathbf{u}, \boldsymbol{\beta}, \mathbf{b})$ , with joint expectation  $\boldsymbol{\mu}_x$  and precision  $\mathbf{Q}_x$ :

$$(\mathbf{x} \mid \boldsymbol{\theta}) \sim \mathcal{N}(\boldsymbol{\mu}_x, \mathbf{Q}_x^{-1}) \quad (\text{Prior})$$

$$(\mathbf{y} \mid \mathbf{x}, \boldsymbol{\theta}) \sim \mathcal{N}(h(\mathbf{x}), \mathbf{Q}_{y|\mathbf{x}}^{-1}) \quad (\text{Observations})$$

$$p(\mathbf{x} \mid \mathbf{y}, \boldsymbol{\theta}) \propto p(\mathbf{x} \mid \boldsymbol{\theta}) p(\mathbf{y} \mid \mathbf{x}, \boldsymbol{\theta}) \quad (\text{Conditional posterior})$$

## Non-linear and/or non-Gaussian observations

For a non-linear  $h(\mathbf{x})$  with Jacobian  $\mathbf{J}$  at  $\mathbf{x} = \boldsymbol{\mu}^*$ , iterate:

$$(\mathbf{x} \mid \mathbf{y}, \boldsymbol{\theta}) \stackrel{\text{approx}}{\sim} \mathcal{N}(\tilde{\boldsymbol{\mu}}, \tilde{\mathbf{Q}}^{-1}) \quad (\text{INLA posterior from } \bar{h}(\mathbf{x}) = h(\boldsymbol{\mu}^*) + \mathbf{J}(\mathbf{x} - \boldsymbol{\mu}^*))$$

$$\tilde{\mathbf{Q}} = \mathbf{Q}_x + \mathbf{J}^\top \mathbf{Q}_{y|\mathbf{x}} \mathbf{J} \quad (\text{Generally: } \mathbf{Q}_x - \nabla_x \nabla_x^\top \log p(\mathbf{y}|\mathbf{x}, \boldsymbol{\theta}))$$

$$\boldsymbol{\mu}_{\text{new}}^* = \boldsymbol{\mu}^* + (\tilde{\boldsymbol{\mu}} - \boldsymbol{\mu}^*) \cdot \underset{a>0}{\text{argmin}} \|\bar{h}(\tilde{\boldsymbol{\mu}}) - h(\boldsymbol{\mu}^* + (\tilde{\boldsymbol{\mu}} - \boldsymbol{\mu}^*)a)\|$$

# References

- ▶ Rue, H. and Held, L.: Gaussian Markov Random Fields; Theory and Applications; *Chapman & Hall/CRC*, 2005
- ▶ Lindgren, F.: Computation fundamentals of discrete GMRF representations of continuous domain spatial models; preliminary book chapter manuscript, 2015,  
<https://www.maths.ed.ac.uk/~flindgre/cuso2019/gmrf.pdf>
- ▶ Lindgren, F., Rue, H., and Lindström, J.: An explicit link between Gaussian fields and Gaussian Markov random fields: the stochastic partial differential equation approach (with discussion); *JRSS Series B*, 2011  
R packages: INLA (<http://r-inla.org/>)  
and inlabru (<https://inlabru-org.github.io/inlabru/>)
- ▶ Lindgren, F., Bolin, D., and Rue, H.: The SPDE Approach for Gaussian and Non-Gaussian Fields: 10 Years and Still Running; *Spatial Statistics, Special Issue: The Impact of Spatial Statistics*, 50:100599, 2022.  
<https://arxiv.org/abs/2111.01084>
- ▶ Lindgren, F., Haakon Bakka, David Bolin, Elias Krainski, Håvard Rue: A diffusion-based spatio-temporal extension of Gaussian Matérn fields, arXiv 2020–2023. <https://arxiv.org/abs/2006.04917>
- ▶ Video illustrating the results, produced by Philip Brohan:  
<https://twitter.com/philipbrohan/status/1253411283598073867>  
<https://player.vimeo.com/video/403663259>
- ▶ Links to EUSTACE project reports and data:  
<https://www.eustaceproject.org/>



# Standardised observation uncertainty models

- ▶ Each data source may have complicated dependence structure
- ▶ To facilitate information blending, use a common error term structure

## Common satellite derived data error model framework

The observational&calibration errors are modelled as three error components:

- ▶ independent ( $\epsilon_0$ ),
- ▶ spatially and/or temporally correlated ( $\epsilon_1$ ), and
- ▶ systematic ( $\epsilon_2$ ),

with distributions determined by the uncertainty information from satellite calibration models.

$$\text{E.g., } y_i = T_m(\mathbf{s}_i, t_i) + \epsilon_0(\mathbf{s}_i, t_i) + \epsilon_1(\mathbf{s}_i, t_i) + \epsilon_2(\mathbf{s}_i, t_i)$$

In practice, each data source might have several different components of each type; independent components can be merged, but not necessarily correlated or systematic components.